Large uncertainty in carbon uptake potential of land-based climate-change mitigation efforts

Andreas Krause, Thomas A.M. Pugh, Anita D Bayer, Wei Li, Felix Leung, Alberte Bondeau, Jonathan C. Doelman, Florian Humpenöder, Peter Anthoni, Benjamin L Bodirsky, et al.

MR. ANDREAS KRAUSE (Orcid ID : 0000-0003-3345-2989)

DR. WEI LI (Orcid ID : 0000-0003-2543-2558)

DR. CHRISTOPH MÜLLER (Orcid ID : 0000-0002-9491-3550)

Article type : Primary Research Articles

Title page

Title: Large uncertainty in carbon uptake potential of land-based climate-change mitigation efforts

Running head: Large uncertainty in carbon uptake potential

List of authors: Andreas Krause[1], Thomas A. M. Pugh[1,2], Anita D. Bayer[1], Wei Li[3], Felix Leung[4], Alberte Bondeau[5], Jonathan C. Doelman[6], Florian Humpenöder[7], Peter Anthoni[1], Benjamin L. Bodirsky[7], Philippe Ciais[3], Christoph Müller[7], Guillermo Murray-Tortarolo[4,8], Stefan Olin[9], Alexander Popp[7], Stephen Sitch[4], Elke Stehfest[6], Almut Arneth[1]

Institute or laboratory of origin: [1]Karlsruhe Institute of Technology, Institute of Meteorology and Climate Research – Atmospheric Environmental Research (IMK-IFU), Kreuzeckbahnstr. 19, 82467 Garmisch-Partenkirchen, Germany

[2]School of Geography, Earth & Environmental Sciences and Birmingham Institute of Forest Research, University of Birmingham, B15 2TT, United Kingdom

doi: 10.1111/gcb.14144

[3]Laboratoire des Sciences du Climat et l'Environnement, CEA-CNRS-UVSQ, Gif-sur-Yvette, France

[4]College of Life and Environmental Sciences, University of Exeter, Exeter, United Kingdom

[5]Institut Méditerranéen de Biodiversité et d'Ecologie marine et continentale (Mediterranean Institute for Biodiversity and Ecology, IMBE), Aix-en-Provence, France

[6]Department of Climate, Air and Energy, Netherlands Environmental Assessment Agency (PBL), PO Box 30314, 2500 GH The Hague, Netherlands

[7]Potsdam Institute for Climate Impact Research (PIK), Telegrafenberg, PO Box 60 12 03, 14412 Potsdam, Germany

[8]Catedra CONACyT comisionado al Instituto de Investigaciones en Ecosistemas y Sustentabilidad, Universidad Nacional Autonoma de Mexico, Mexico

[9]Department of Physical Geography and Ecosystem Science, Lund University, 22362 Lund, Sweden

Corresponding author's telephone and email details: ++49 8821 183186, andreas.krause@kit.edu

Keywords: carbon dioxide removal, negative emissions, land-based mitigation, BECCS, avoided deforestation and afforestation

Paper type: Primary Research Article

Abstract

Most climate mitigation scenarios involve negative emissions, especially those that aim to limit global temperature increase to 2°C or less. However, the carbon uptake potential in land-based climate change mitigation efforts is highly uncertain. Here, we address this uncertainty by using two land-based mitigation scenarios from two land-use models (IMAGE and MAgPIE) as input to four dynamic global vegetation models (DGVMs; LPJ-GUESS, ORCHIDEE, JULES, LPJmL). Each of the four combinations of land-use models and mitigation scenarios aimed for a cumulative carbon uptake of ~130 GtC by the end of the century, achieved either via the cultivation of bioenergy crops combined with carbon capture and storage (BECCS) or avoided deforestation and afforestation (ADAFF).

Results suggest large uncertainty in simulated future land demand and carbon uptake rates, depending on the assumptions related to land use and land management in the models. Total cumulative carbon uptake in the DGVMs is highly variable across mitigation scenarios, ranging between 19 and 130 GtC by year 2099. Only one out of the 16 combinations of mitigation scenarios and DGVMs achieves an equivalent or higher carbon uptake than achieved in the land-use models. The large differences in carbon uptake between the DGVMs and their discrepancy against the carbon uptake in IMAGE and MAgPIE are mainly due to different model assumptions regarding bioenergy crop yields, and due to the simulation of soil carbon response to land-use change. Differences between land-use models and DGVMs regarding forest biomass and the rate of forest regrowth also have an impact, albeit smaller, on the results. Given the low confidence in simulated carbon uptake for a given land-based mitigation scenario, and that negative emissions simulated by the DGVMs are typically lower

than assumed in scenarios consistent with the 2°C target, relying on negative emissions to mitigate climate change is a highly uncertain strategy.

Introduction

"Negative emissions", i.e. the removal of carbon dioxide (CDR) from the atmosphere, is an important concept for climate change mitigation (Lenton and Vaughan, 2009). Scenarios based on land-use (LU) models or Integrated Assessment Models (IAMs) tend to achieve an end-of-century warming goal at or below 2°C only through negative emissions which commence within the next 1-2 decades, and then increase and are sustained at considerable rates during the second half of the 21st century (Anderson and Peters, 2016, Fuss *et al.*, 2014, Gasser *et al.*, 2015, Riahi *et al.*, 2017, Rogelj *et al.*, 2015, Sanderson *et al.*, 2016, Smith *et al.*, 2016a). So far, negative emissions represented in IAMs are mainly land-based options (Popp *et al.*, 2017, Popp *et al.*, 2014b).

IAMs currently focus on two land-based CDR technologies which both utilize the carbon (C) uptake by plants via photosynthesis. One is large-scale cultivation of crops or trees for bioenergy and capturing the C released upon combustion for long-term storage in geologic formations (BECCS). The other is to maintain or increase terrestrial C stocks via avoided deforestation and afforestation/reforestation (ADAFF). These are the two most widely-used options in IAMs to achieve negative emissions because they do not have to rely on the development of new, large-scale technology (ADAFF), or are regarded as the most prolific option with the capability to supply energy (BECCS) (Humpenöder *et al.*, 2014, Smith *et al.*, 2016a). However, the land demand/availability of these approaches is highly uncertain

(Boysen *et al.*, 2017a, Popp *et al.*, 2017), and their potential to remove significant amounts of C from the atmosphere is regarded as controversial (Fuss *et al.*, 2014). Additionally, conflicts with other LU, associated supply of ecosystem services, and maintenance/enhancement of biodiversity are highly likely (Krause *et al.*, 2017, Smith *et al.*, 2016a, Williamson, 2016). Considering typical time frames of decades involved in the planning and establishment of climate mitigation projects, the quantification of their uncertainties in terms of achievable CDR is important to inform policy makers about practicality and risks.

Here, we address the uncertainty of C uptake potential from land-based climate change mitigation by using projections of future land-use change (LUC) from one IAM (IMAGE) and one socio-economic LU model (MAgPIE; for simplicity we refer to IMAGE and MAgPIE as land-use models - LUMs - in the following) as input to four dynamic global vegetation models (DGVMs; LPJ-GUESS, ORCHIDEE, JULES, LPJmL). In these scenarios, C uptake is achieved either via BECCS or via ADAFF. The cumulative additional C uptake target in each mitigation LUC scenario is 130 GtC by year 2100 compared to a baseline LUC scenario without additional land-based mitigation (BASE). We analyze total C uptake and the relative contribution of vegetation, soils, and C storage via CCS in the four DGVMs and compare it to the C uptake targeted and achieved in the LUMs.

Materials and methods

Detailed information about the LUMs and the scenarios can be found in Krause et al. (2017). In the following we provide a short description of the LUMs and the scenarios.

Description of the land-use models

The Integrated Model to Assess the Global Environment (IMAGE) is an ecological-environmental model framework simulating the environmental consequences of human activities worldwide (Stehfest et al., 2014).

The Model of Agricultural Production and its Impact on the Environment (MAgPIE) is a global LU and agro-food system model. It optimizes spatial-explicit LU patterns and intensification levels to satisfy a given food, feed, material, and bioenergy demand at minimal production costs (Lotze-Campen *et al.*, 2008, Popp *et al.*, 2014a).

Climate change and CO_2 impacts on forest growth and crop yields are accounted for in the LUMs. The LPJmL DGVM (Bondeau *et al.*, 2007) represents the crop/vegetation sub-model in both IMAGE (where it is dynamically coupled) and MAgPIE (where it provides potential C stocks, crop yields, irrigation water requirements, and blue water availability as input data). We also use an offline version of LPJmL as one of our four DGVMs which differs from the versions used in the LUMs mainly by not considering technological yield increases in the future.

Land-use scenarios

Both LUMs harmonized their pasture and cropland LU patterns to the HYDE 3.1 dataset (Klein Goldewijk *et al.*, 2011) in the years 2005 (IMAGE) or 1995 (MAgPIE) to create a continuous historical-to-future time series. The simulation period was 1970-2100 for IMAGE

and 1995-2100 for MAgPIE, with LUC scenarios starting to diverge in year 2005. The spin-up in IMAGE was set to 700 years with natural vegetation cover followed by 300 years with year 1970 land-cover map, climate and CO_2. In MAgPIE, potential C densities from LPJmL were used as initial (1995) values, with agricultural vegetation and litter C set to zero and soil C depleted based on IPCC recommendations to account for real land cover at the start of the simulation period (Humpenöder *et al.*, 2014). Socioeconomic developments as input to the LUMs were based on SSP2 (Popp *et al.*, 2017). Food production in the mitigation scenarios was maintained on the same levels as in BASE.

With respect to the rate of forest regrowth in the ADAFF scenarios, MAgPIE parameterizes managed afforestation by climate region specific S-shaped growth curves towards potential forest biomass, and litter and soil C recovering within 20 years (Humpenöder *et al.*, 2014). In contrast, forest regrowth in IMAGE is dynamically simulated by LPJmL, which is a sub-component of IMAGE. This means that similar C uptake rates following afforestation are to be expected for IMAGE and the stand-alone LPJmL DGVM. Forest regrowth in IMAGE partly takes place on degraded forest lands, which are assumed to be completely deforested (Doelman et al., 2018).

The degraded forest land-cover class was implemented in IMAGE due to a mismatch between deforestation rates reported by the FAO's 2015 Forest Resource Assessment (http://www.fao.org/3/a-i4793e.pdf, last accessed September 2017) and historical expansions of cropland and pasture area reported by FAO. These differences are assumed to be caused by additional reasons (e.g. unsustainable forestry preventing regrowth of natural forests, mining,

or illegal logging) and accounted for by a historically calibrated rate of forest degradation, which is extrapolated into the future (Doelman *et al.*, 2018).

Description of the Dynamic Global Vegetation Models

The LUC scenarios were used as input to four DGVMs: LPJ-GUESS (Olin *et al.*, 2015, Smith *et al.*, 2014), ORCHIDEE (Krinner et al., 2005), JULES (Best *et al.*, 2011, Clark *et al.*, 2011), and LPJmL (Bondeau *et al.*, 2007, Sitch *et al.*, 2003). The models have different heritages; while ORCHIDEE and JULES were developed as land components of global climate models (IPSL and UKESM), LPJ-GUESS and LPJmL were originally designed as stand-alone offline models to simulate vegetation dynamics and associated C and water fluxes. All DGVMs represent vegetation using a number of plant functional types (PFTs), with LPJ-GUESS and LPJmL also representing dedicated crop PFTs. LPJ-GUESS is different from the other DGVMs by its explicit representation of forest demography and by having nitrogen cycling as an additional constraint on ecosystem C processes (in addition to soil water availability which is accounted for in all DGVMs). All DGVMs represent LUC and land management explicitly even though the models differ in terms of implemented processes and level of detail. Table 1 and the extended Table S1 provide an overview of model differences which are important for this study.

Simulation setup

The DGVM simulation period was 1901-2099. DGVMs were first spun up to pre-industrial equilibrium state (1901), recycling 1950-1959 climatology to attain a stable equilibrium of C pools and fluxes in each model using atmospheric CO_2 concentration from 1901

(Meinshausen et al., 2011). Climate from the 1950-1959 period was used for the spin-up because these were the first years in the climate data set, a common practice in this kind of set-up. DGVMs were then applied over the transient period 1901-2099 using transient CO_2 (Meinshausen *et al.*, 2011) and climate data (1950-2099) simulated by the IPSL-CM5A-LR climate model for the representative concentration pathway RCP2.6 from the ISI-MIP project, bias-corrected as in Hempel et al. (2013). The temperature increase is 2°C by the end of the 21st century relative to the pre-industrial era. The climate data for the spin-up and the 1901-1949 period were randomly taken from the 1950-1959 period. Future atmospheric CO_2 mixing ratio followed the RCP2.6 pathway, peaking at 443 ppmv in year 2052 (Meinshausen *et al.*, 2011). LUC was based on spatially explicit LU maps derived from the LUMs (for the historic period based on HYDE3.1) and translated into the vegetation types of each DGVM (see Table 1). The DGVMs aimed to be as consistent as possible with the LUMs when implementing LU patterns from the LUM scenarios, e.g. for IMAGE scenarios all DGVMs apart from JULES followed the IMAGE assumption of degraded forests being grasslands. Management information (crop types, irrigation, and nitrogen fertilizers) were also provided by the LUMs but were only used by some DGVMs which represented the relevant processes explicitly (Table 1). LPJ-GUESS was the only model being able to use nitrogen fertilizers as provided by the LUMs. Nitrogen application rates (synthetic plus manure) were available from 1970/1995 on. They were derived to match assumed crop yields in the LUMs. A historic hindcast (1901-1969/1901-1994) was calculated based on initial (1970/1995) fertilizer rates from the LUMs and relative changes in the Land-Use Harmonization data set (http://luh.umd.edu/index.shtml, see also Krause et al., 2017). The implementation of the LU data into the DGVMs (e.g. mapping to DGVM vegetation types and defining rules by which managed land expands over natural vegetation), land masks, and additional required input variables (e.g. soil characteristics) were left to the responsibility of the individual DGVM

groups. Different model structures and implementations of the LU patterns can result e.g. in differences in global forest area in the individual DGVMs (Fig. S1). The spatial resolution of the DGVMs was the same as the resolution of the input data (0.5°x0.5°), except for ORCHIDEE (2°x2°). In total, 24 combinations of DGVMs and LUC scenarios were simulated, including 16 combinations of DGVMs and mitigation LUC scenarios.

Results

Land-use scenarios

In both LUMs, LUC is generally greater for ADAFF scenarios than for BECCS scenarios (Fig. S2) because the former is simulated with LUMs to be less efficient at CDR than the latter (Humpenöder, et al., 2014). The different C accumulation trajectories in ADAFF (see methods) result in ADAFF activities starting earlier in IMAGE but avoided deforestation/afforestation area being slightly larger in MAgPIE by the end of the century (Figs. S1, S2a,b, Table S2). Forest area by year 2099 is 1040 Mha larger in ADAFF than in BASE for IMAGE and 1103 Mha larger for MAgPIE. For IMAGE, ~42% of this difference in forest area can be attributed to avoided deforestation and 58% to afforestation. For MAgPIE, the corresponding numbers are only 4% for avoided deforestation and 96% for afforestation, emphasizing the much larger role of afforestation compared to avoided deforestation in MAgPIE. The LUMs also differ in terms of land-cover classes affected by ADAFF activities. In IMAGE, forest maintenance and expansion usually takes place on pastures or degraded forests (ADAFF compared to BASE), but in MAgPIE afforestation on abandoned croplands is also relevant, particularly after year 2070 (see Table S2; note that some of the abandoned cropland in MAgPIE ADAFF is not afforested but instead converted

to pasture while at other locations pastures are converted to forests, resulting in small net changes in pasture area by the end of the century).

The area needed for bioenergy production is mainly taken from natural vegetation in IMAGE but also from existing agricultural land in MAgPIE. IMAGE has a larger bioenergy land demand to fulfil the same CCS target as MAgPIE (Fig. S2c,d). This reflects different modelling approaches: in IMAGE, land allocation for bioenergy cultivation follows a rule-based approach according to sustainability criteria, implying that only marginal land not needed for food production is available for bioenergy. In MAgPIE, bioenergy and food production compete for fertile land based on a cost minimization procedure. Consequently, average bioenergy yields are lower in IMAGE than in MAgPIE, thereby increasing the required area to deliver the same annual CCS rates.

Present-day carbon pools and future changes in the baseline scenarios

Present-day C pools as simulated by IMAGE and MAgPIE are 440 and 484 GtC in global vegetation, and 1121 and 1981 GtC in the soils (including litter), respectively. The large divergence in soil C between the two LUMs is likely mainly due to the representation of permafrost in MAgPIE. Vegetation C simulated by the DGVMs ranges between 275 and 425 GtC, and soil C between 1315 and 1954 GtC (Fig. S3). For the two non-mitigation BASE scenarios, in all DGVMs except LPJmL the land acts as a net C sink between year 2000 and 2099 (Fig. S3). The magnitude and direction of change in C pools is determined by the DGVM's response to RCP2.6 climate change, CO_2 fertilization, and baseline LUC.

Total carbon uptake in the mitigation scenarios

Total additional C uptake in the mitigation scenarios is here calculated as the sum of changes in vegetation C, litter and soil C, and (relatively negligible) product pool C, plus cumulative CCS (all relative to BASE). While an uptake target of 130 GtC was set in both LUMs, actual C uptake in the LUMs in most cases deviates somewhat from this number. For the ADAFF scenarios, the simplicity of the afforestation implementation in IMAGE was unable to exactly meet the target. In MAgPIE, afforestation decision-making was based on present-day potential C pools. Potential impacts of climate change on the terrestrial C storage capacity were therefore not considered which leads to a mismatch between intended and actual sequestration. The realized C uptake in ADAFF between year 2005 and 2099 is 141 GtC in IMAGE and 120 GtC in MAgPIE (Figs. 1a,b, 2a). Around 49% of the total C increase in IMAGE ADAFF can be attributed to avoided deforestation and 51% to afforestation (for MAgPIE spatial C stocks were not available but afforestation is certainly much more important due to the limited decline in forest area in MAgPIE BASE). For BECCS, in both LUMs the CDR target was implemented as a gross CCS target which included the harvested C from bioenergy crops and a fractional (80%; Klein et al., 2014) capture and storage of this harvest. Cumulative CCS reaches 128 GtC in year 2099 in both LUMs (see subsection "Cumulative CCS") so the implemented CDR/CSS target is achieved. However, calculations of the target in the LUMs originally neglected terrestrial C losses from deforestation for bioenergy cultivation. When these are included, cumulative CCS combined with ecosystem C losses from deforestation result in a net total C uptake of 86 and 107 GtC, thus below the sought target due to emissions from LUC.

In contrast to the two LUMs, total C uptake (relative to BASE) is typically lower in the DGVM simulations forced by the same LU patterns, with total C uptake in the DGVMs ranging between 19 and 130 GtC (Figs. 1a,b, 2a). Unsurprisingly (as LPJmL represents the vegetation component of the LUMs), the closest agreement exists between the LUMs and LPJmL. ORCHIDEE simulates the lowest uptake for ADAFF and JULES the lowest uptake for BECCS. The maximum yearly total C uptake per decade within the 21st century ranges from 1.9 GtC yr^{-1} (IMAGE ADAFF) to 3.5 GtC yr^{-1} (MAgPIE ADAFF) in the LUMs and from 0.4 GtC yr^{-1} (ORCHIDEE IMAGE-ADAFF) to 2.0 GtC yr^{-1} (LPJmL IMAGE-BECCS) in the DGVMs. Spatially, total C uptake is concentrated in the tropics for ADAFF (except in ORCHIDEE, which simulates substantial emissions in some regions), while patterns are more diverse for BECCS (Fig. 3). The largest agreement in total C uptake across DGVMs is found in tropical Africa for the ADAFF scenarios (Fig. S4). The contributions of vegetation, soil, and cumulative CCS to model discrepancies in total C uptake are analyzed in the following subsections.

Vegetation carbon

As intended, the simulations with the ADAFF scenarios result in increasing biomass over the 21st century compared to the BASE simulations for all LUMs and DGVMs. Vegetation C uptake in year 2099 is 79 and 66 GtC in IMAGE and MAgPIE and ranges between 39 and 73 GtC in the DGVMs (Figs. 1c,d, 2b), with generally larger uptake for IMAGE scenarios than for MAgPIE scenarios due to the earlier start of ADAFF activities in IMAGE (Table S2). Biomass accumulation occurs at a relatively steady rate in the DGVMs but accelerates during the second half of the century in the LUMs (Fig. 1c,d). There is a drop in vegetation C for LPJmL MAgPIE-ADAFF around mid-century. As agricultural land has low vegetation C

pools in LPJmL this is related to a decreasing vegetation C density in forests, which is not compensated for by the simultaneous increase in forest area. Tree PFTs in LPJmL are represented by average individuals (representing all trees belonging to this PFT), and the individual's properties are changed when afforestation occurs in a grid-cell. These changes in the PFT's properties might in some regions reduce its ability to compete or make it more vulnerable to disturbances so that tree mortality is increased compared to the BASE scenario in which no afforestation took place.

The vegetation C uptake in IMAGE can be equally attributed to avoided deforestation and to afforestation (Table S3). No quantification is possible in MAgPIE because spatial C stocks were not available. In the DGVMs, the contribution of avoided deforestation to the vegetation C uptake in ADAFF is generally larger for IMAGE-LU than for MAgPIE-LU (Table S3), confirming the much larger role of afforestation compared to avoided deforestation in MAgPIE. For BECCS, all LUMs and DGVMs simulate deforestation-driven decreases in vegetation C. JULES simulates the largest biomass losses upon deforestation and ORCHIDEE the smallest losses. Since global vegetation C stocks are similar across DGVMs (with the exception of ORCHIDEE, Fig. S3), differences in C losses arise from spatial variations in biomass which DGVMs (and presumably LUMs) are known to not capture well (Johnson et al., 2016). BECCS deforestation emissions are generally larger for IMAGE-LU patterns than for MAgPIE-LU patterns, reflecting the much larger decline in forest area (Fig. S1, Table S2).

Site-level comparisons can help us to better understand differences across models. Therefore, in order to understand local responses better and to use these to interpret the simulated global totals, we extracted grid-cells from the global simulations (for IMAGE scenarios as spatial information were not available from MAgPIE), selected because a large fraction of the grid-cells' area underwent land-cover transitions within the 21st century. However, there are substantial variations in the models' response to LUC across different sites, making it difficult to choose representative grid-cells and to draw universal conclusions from this comparison. Figure S5 shows three relatively representative example sites. As expected for a 0.5° resolution, there are substantial differences on grid-cell level across models in terms of initial vegetation C densities. All models simulate increasing biomass in response to afforestation (Fig. S5a,b) and biomass losses upon deforestation (Fig. S5c). However, JULES does not simulate forest degradation (Fig. S5c; see methods for more information about degraded forests), contributing to the lower vegetation C uptake compared to the other DGVMs for the IMAGE ADAFF scenario.

For MAgPIE scenarios, site-level comparisons are not shown because MAgPIE only reported global C pools. For the MAgPIE ADAFF scenario, global vegetation C uptake is very similar in all DGVMs but lower than in MAgPIE (Fig. 1d). It seems that one reason for this divergence is different assumptions about potential vegetation C stocks (available for MAgPIE and LPJ-GUESS; see Fig. S6). An additional factor explaining the divergence is the pace of the regrowth curve. In contrast to the other models, MAgPIE assumes a single response function per biome, irrespective of spatial differences in climate and soil conditions within a biome, and thus ignores the effects of spatial differences within a biome, e.g. in terms of annual precipitation or soil fertility on forest regrowth (Poorter *et al.*, 2016). Additionally, MAgPIE does not account for disturbances. When looking at forest regrowth

rates averaged over different biomes it seems that tropical regrowth occurs much faster in MAgPIE than, for example, in LPJ-GUESS (Fig. S7a).

Soil carbon

Compared to vegetation, modelled soil C changes in response to ADAFF activities are much more diverse, with some DGVMs simulating net soil C losses upon afforestation (Figs. 1e,f, 2c). Soil C uptake in ADAFF is 62 GtC in IMAGE and 54 GtC in MAgPIE, which is comparable to vegetation C uptake. In contrast, soil C changes in the DGVMs range between -33 and +57 GtC. Soil C accumulation in LPJmL for the MAgPIE ADAFF scenario starts significantly earlier than in the other models. As afforestation on pastures is common in MAgPIE until around year 2070, this indicates a large soil C uptake potential in LPJmL for pasture-forests transitions, which is also apparent in the LPJmL simulations driven by the IMAGE ADAFF LU patterns. For BECCS, all models simulate small soil C losses (up to -16 GtC) which are generally larger in the LUMs than in the DGVMs. In both ADAFF and BECCS, differences between LUMs and DGVMs in terms of soil C changes are more pronounced for IMAGE-LU patterns than for MAgPIE-LU patterns.

The soil C emissions in JULES and ORCHIDEE for the ADAFF scenarios (and the relatively low emissions for BECCS) might be partly caused by the simplistic representation of agricultural management processes in these models. While LPJmL and LPJ-GUESS represent croplands by specific crop PFTs and growing seasons, ORCHIDEE and JULES grow crops as harvested grass (modified natural grass in ORCHIDEE, natural grass in JULES; see Table 1). Additionally, ORCHIDEE does not include grazing of pastures, which means more

biomass C is transferred to the litter when the grass dies. Consequently, pastures and croplands have larger soil C pools in ORCHIDEE and JULES, respectively, than if these processes were accounted for, resulting in less soil C accumulation potential upon afforestation. To test further how different representations of agriculture in the DGVMs affect soil C changes upon afforestation we performed two sensitivity simulations with LPJ-GUESS in which we simplified the representation of management processes following Pugh et al. (2015). In these simulations, the rate of change in LPJ-GUESS soil C pools is reduced by 57% in the MAgPIE ADAFF scenario (compared to the "standard" LPJ-GUESS simulations) when croplands are represented by pastures (mimicking the representation of croplands in JULES), and by 49% in the IMAGE ADAFF case when pastures are not harvested (mimicking the representation of pastures in ORCHIDEE, not shown). Furthermore, LPJ-GUESS, JULES, and particularly ORCHIDEE simulate a widespread decline in net primary productivity (NPP) upon afforestation (Figs. 2f, S8) because in these models tropical grasslands (or croplands) are often more productive than tropical forests. LPJmL, on the other hand, accounts for regional yield gaps so cropland NPP is scaled down. Even though the fraction of NPP transferred to the soil might differ across models (e.g. due to different mortality in secondary forests), this suggests that the lower productivity of re-growing forests compared to agriculture also plays an important role for the limited soil C accumulation (or emissions) in LPJ-GUESS, JULES, and ORCHIDEE.

Cumulative CCS

CCS is calculated by multiplying the harvested C of bioenergy crops by a capture efficiency of 80% before geologic storage. A prescribed CCS trajectory was implemented in both LUMs, which means that annual global CCS rates are the same in IMAGE and MAgPIE.

Cumulative CCS reaches 128 GtC in both LUMs by year 2099. In the DGVMs, cumulative CCS ranges from 37 to 130 GtC by year 2099 (Figs. 1g,h, 2d).

As the DGVMs used bioenergy production area from the LUMs and also the same assumptions about capture efficiency and storage capacity, the lower CCS calculated in most of the DGMVs has to arise mainly from differences in simulated bioenergy yields, including differences in the harvest index. Both LUMs assume rain-fed perennial and fast-growing second generation bioenergy crops (such as Miscanthus) to fulfil the CCS demand. LPJmL is the only DGVM representing dedicated bioenergy crops explicitly, but like the other DGVMs does not assume technological yield increases. This implies that the slightly larger cumulative CCS than in MAgPIE originates from higher initial yields. In contrast, LPJ-GUESS grows bioenergy as maize (with residues included for CCS), ORCHIDEE as crop grass, and JULES as natural grass (for harvest assumptions see Table S1). Consequently, average bioenergy yields are highest in LPJmL followed by LPJ-GUESS and then ORCHIDEE and JULES (Fig. S9). Cumulative CCS in all DGVMs apart from LPJmL is higher for IMAGE-LU patterns than for MAgPIE-LU patterns (Figs. 1g,h, 2d) because the larger cultivation area in IMAGE (Fig. S2c,d) outweighs lower average yields (Fig. S9). In the LUMs, the same trade-off between land expansion and yields results in equivalent global CCS rates in both LUMs.

Discussion

The C uptake potential of afforestation is largely restricted by historic C removal via deforestation. Cumulative LUC emissions over the 1750-2015 period were ~190 GtC (Le Quere et al., 2016), with a very large uncertainty arising from how different forms of land

management are considered in the simulations (Arneth et al., 2017) but also due to different LUC hindcasts (Bayer et al., 2017). However, a possibly large fraction of agricultural area will be needed for future food production (Boysen *et al.*, 2017a, Popp *et al.*, 2017) and CO_2 fertilizing effects on forest growth will likely be limited in RCP2.6. This suggests that achieving 130 GtC net uptake via ADAFF might be challenging, consistent with results from the DGVMs here (especially for MAgPIE-LU where avoided deforestation only plays a minor role compared to afforestation). A limited (<150 GtC) C uptake potential via afforestation within this century was also estimated in previous studies, despite very different methods and assumptions (Lenton, 2010, and references therein). However, one recent study (Sonntag *et al.*, 2016) found a much larger (215 GtC) uptake in a coupled Earth System Model (ESM) for a high emission scenario (RCP8.5) when using RCP4.5 LU (afforestation, -700 Mha agricultural land) instead of RCP8.5 LU (deforestation, +800 Mha agricultural land). The C uptake was thus higher than in our study, but so were baseline deforestation rates, climate impacts, and, particularly, differences in CO_2 fertilization (RCP8.5 *vs.* RCP2.6 in our study); the high levels of CO_2 fertilization under RCP8.5 typically causes DGVMs to simulate much larger C uptake in forests.

Some of the discrepancy in total C uptake between the LUMs and the DGVMs in the ADAFF scenarios originates from differences in vegetation C uptake, especially for MAgPIE. Natural forest regrowth upon agricultural abandonment is implemented in all DGVMs and IMAGE, while MAgPIE assumes managed regrowth according to prescribed, region-specific growth curves towards the biomass density of potential natural vegetation (Humpenöder *et al.*, 2014). Observational studies differ substantially in reported forest regrowth rates (Krause *et al.*, 2016, and references therein). Biomass accumulation in tropical forests has often been reported to slow down a few decades after agricultural cessation, with aboveground biomass

levels (representing ~80% of total biomass, Cairns *et al.*, 1997) of mature tropical forests being reached within ca. 66-90 years (Anderson-Teixeira *et al.*, 2016, Poorter *et al.*, 2016), and belowground biomass needing more time to recover, especially following shifting agriculture (Martin *et al.*, 2013). Poorter et al. (2016) also found slower accumulation rates in dry (<1500 mm) compared to wet (>2500 mm) environments. In comparison, tropical (22°S-20°N as in Poorter et al.) afforestation in the MAgPIE ADAFF scenario occurs in relatively dry regions, with an average precipitation of 1682 mm yr^{-1}. While we can only quantify tropical recovery times (90% of old forest biomass) for MAgPIE (47 years; Fig. S7a) and LPJ-GUESS (~150 years in tropical Africa), the vegetation C uptake is similar across all DGVMs. The observational studies point towards typical recovery times that lie in the middle of this range. This suggests that, assuming that afforestation will mostly occur as natural regrowth, tropical biomass accumulation rates might be overestimated in MAgPIE. The LPJ-GUESS recovery times of Krause et al. (2016) are, however, not directly comparable to these observations, as the LPJ-GUESS simulations allowed natural stand-replacing disturbances (e.g. fire, wind-throw) to occur in these recovering forests, slowing the recovery rate, whilst this is not likely to be the case in the chronosequence observations, which typically age the stand from last disturbance. Evaluation of forest regrowth rates in DGVMs, particularly in tropical forests, will be important to constrain uncertainty in ADAFF potential.

Degraded forests also represent an uncertainty in our IMAGE scenarios. JULES represented degraded forests as natural vegetation, whereas the other DGVMs, simply for consistency, followed the IMAGE assumption of degraded forests being grassland. In reality, degraded forests likely represents a mixture between both approaches, with aboveground biomass on average being 70% lower than in undisturbed forests (Asner et al., 2010). Clearly, assuming a degraded forest being a grassland will overestimate vegetation C uptake potential when

degraded forests are converted back to forests (in IMAGE ~50% of the avoided deforestation and afforestation area by end-century is from degraded forests; see Table S2). Additionally, the mismatch between forest loss and agricultural gain reported by FAO (based on which the degraded forest class was introduced in IMAGE) might be largely explained by shifting cultivation (Houghton and Nassikas, 2017). However, most LUMs/DGVMs so far cannot adequately simulate shifting cultivation due to not explicitly representing forest demography. The representation of forest degradation thus remains a challenge for LUMs and DGVMs.

Soil C changes contribute most to variations in total C uptake across models. Differences in simulated present-day soil C stocks are hardly surprising as global soil C estimates are very uncertain (Scharlemann *et al.*, 2014) and large variations across DGVMs and ESMs have been reported before (Anav *et al.*, 2013, Tian *et al.*, 2015, Todd-Brown *et al.*, 2013). Numerous studies explored soil C changes following LUC (Smith *et al.*, 2016b, and references therein), but there is still substantial disagreement in terms of the magnitude of change for most land-cover transitions. While studies agree that transitions from forests to croplands reduce soil C (and vice versa), patterns are more diverse for conversions to/from grassland, depending on management intensity, climate, and soils (McSherry and Ritchie, 2013, Powers *et al.*, 2011). The picture is further complicated by evidence that the existing field observations in the tropics might not be representative for many tropical landscapes (Powers *et al.*, 2011).

The LUC scenarios from the LUMs differ in terms of converted land-cover types: in MAgPIE, afforestation partly takes place on former croplands (especially before year 2025 and after 2070). MAgPIE assumes initial litter C (both in croplands and pastures) to be

completely depleted and, based on IPCC guidelines, to be replenished within 20 years following agricultural abandonment. Soil C in former croplands is assumed to increase from the grid-cell specific average soil C density of cropland and natural vegetation towards the soil C density of natural vegetation within 20 years (Humpenöder *et al.*, 2014). However, a litter C density of zero and an assumed time frame of 20 years until soil C reaches equilibrium appear questionable. In fact, some studies report soil C to decrease during the first years after cropland cessation (Deng *et al.*, 2016), and subsequent C accumulation is usually slow and proceeds over several decades or even centuries (Silver *et al.*, 2000). In contrast to the prescribed recovery implemented in MAgPIE, IMAGE simulates soil C changes dynamically within LPJmL. However, the contribution of soils to total C uptake is comparable to MAgPIE even though ADAFF activities in IMAGE are largely restricted to pasture-forest transitions. In reality, afforestation on grasslands (or avoided conversion from forests to grasslands) has even less soil C uptake potential than on croplands; soil C depletions in pastures/grasslands relative to forests are generally low (Don *et al.*, 2011, Laganiere *et al.*, 2010) and in many cases grasslands even store more soil C than the replacing forests (Li et al., submitted; Guo and Gifford, 2002, Poeplau *et al.*, 2011, Powers *et al.*, 2011). Additionally, declines in soil C have been reported during the first years of forest regrowth before accumulation occurs and net accumulation is often only achieved after several decades (Paul *et al.*, 2002, Poeplau *et al.*, 2011). Consequently, the rapid soil C uptake in the LUMs for ADAFF is likely overoptimistic, while limited soil C accumulation (compared to vegetation C) in response to afforestation as simulated by some DGVMs seems to be more realistic. However, historic agriculture has likely resulted in substantial net soil C emissions (Sanderman *et al.*, 2017, Smith *et al.*, 2016b), so large soil C losses in response to afforestation as simulated by ORCHIDEE are also unlikely, especially for the MAgPIE ADAFF scenario (where croplands are preferentially afforested).

One likely reason for the large discrepancy in simulated soil C changes in response to afforestation is the simulated change in ecosystem productivity. Todd-Brown et al. (2013) showed that soil C stocks in ESMs are closely coupled to simulated NPP. In our simulations, simulated changes in NPP in response to ADAFF activities are very different across models, which partly explains differences in soil C accumulation. Modelling work by DeFries (2002) suggests that regional impacts of LUC on NPP are highly variable, depending on management intensity and original vegetation cover, and that cropland productivity is higher compared to forests in temperate regions. The relatively high productivity of temperate crops seems to be confirmed for European studies (Ciais *et al.*, 2010, Luyssaert *et al.*, 2010), but estimates are highly dependent on the data source from which NPP is derived. In the tropics, observations suggest crop productivity at many locations to be lower than for forests (Cleveland *et al.*, 2015, Monfreda *et al.*, 2008). As afforestation in our scenarios is mostly concentrated in the tropics, the NPP decrease following afforestation in most DGVMs seems to be unrealistic.

A second potentially important reason for the large differences in simulated soil C uptake is different amounts of C removed from agricultural land. Soil C recovery following agricultural cessation has recently been simulated with a different version of LPJ-GUESS (croplands were represented by tilled, fertilized, and harvested grassland rather than specific crop PFTs) and showed reasonable agreement with observations (Krause *et al.*, 2016). ORCHIDEE and JULES represent fewer management processes and therefore may underestimate soil C uptake potential in ADAFF (but also losses in BECCS); the incorporation of harvest (not included in ORCHIDEE pastures) and the representation of crops by specific crop PFTs (including tillage), instead of grasses, substantially increases soil C depletions on agricultural land in LPJ-GUESS (Pugh *et al.*, 2015). However, there are also

observations suggesting that moderately intensive grazing might actually increase soil C stocks in C4-dominated grasslands (McSherry and Ritchie, 2013, Navarrete *et al.*, 2016), a process the DGVMs likely do not capture well.

The LUMs did not include deforestation emissions ("carbon debt", Fargione *et al.*, 2008) in their BECCS CDR target. This is a common procedure in BECCS scenarios (or at least LUC emissions are often not seperated from fossil fuel emissions, e.g. Smith *et al.*, 2016a). For two bioenergy scenarios (600 and 800 Mha production area made available via either deforestation or agricultural abandonment, RCP2.6 climate) comparable in terms of area and climate changes to our scenarios, a modelling study by Wiltshire and Davies-Barnard (2015) estimated vegetation C losses of 70 and 0 GtC and, using average depletions from Guo and Gillford (2002), soil C losses of 20 and 60 GtC. In our simulations, vegetation and soil C emissions are relatively small, but our study still confirms that these emissions should not be neglected when considering bioenergy as an option to achieve negative emissions.

Cumulative CCS in BECCS differs substantially across models, ranging between 37 GtC and 130 GtC in the DGVMs, and reaching 128 GtC in both LUMs. By comparison, Wiltshire and Davies-Barnard (2015) found 75 and 200 GtC for the two comparable scenarios, which is similar to the 100-230 GtC range reported by Smith et al. (2016a) for IAM scenarios consistent with the 2°C target. Recently, Boysen et al. (2017a) estimated land availability for bioenergy production in LPJmL. They found that in the best case scenario, biomass plantations on abandoned agricultural land could deliver up to 350 GtC by 2100 (but likely much less), and potentially more if plantations would replace natural ecosystems. In our study, bioenergy area was prescribed by the LUMs and differences in CCS across models

originate from simulated bioenergy crop yields. The LUMs and LPJmL represent these crops as dedicated bioenergy crops, mimicking characteristics of perennial energy crops like switchgrass or Miscanthus. Bioenergy yields in LPJmL have recently been evaluated against observations and showed reasonable results but were hindered by limited experimental data in the tropics (Heck *et al.*, 2016). The other DGVMs grow bioenergy crops as maize (LPJ-GUESS), productive grass (ORCHIDEE), or natural grass (JULES). JULES and ORCHIDEE also do not increase the harvest index for bioenergy crops relative to food crops. Additionally, the LUMs assume technological yield increases over time, resulting in higher average yields than in most DGVMs. While research of dedicated bioenergy crops is just in its infancy and thus on the one hand promises high potential, there is also evidence that yield increases observed over the last decades for cereals have recently slowed down (Alexandratos and Bruinsma, 2012). In fact, much of the historic yield increase was achieved via increasing the harvest index and fertilizer application, processes that are unlikely to substantially affect bioenergy yields (Searle and Malins, 2014). It also remains to be seen what bioenergy yield will be attainable in more marginal lands compared to sites where these crops are typically grown today (Searle and Malins, 2014). Consequently, what bioenergy yields we can expect in the future is controversial, with the optimistic assumptions made in IAMs/LUMs being plausible, but towards the upper bound of uncertainty (Creutzig, 2016).

We conclude that forest maintenance and expansion, as well as large-scale bioenergy production combined with CCS, offer the potential to remove substantial amounts of C from the atmosphere and thus can help to mitigate climate change. However, the size of the removal is highly uncertain, and may be much less than previously assumed in IAM/LUM scenarios consistent with the 2°C target (Boysen *et al.*, 2017b, Rogelj *et al.*, 2015, Smith *et al.*, 2016a, Tavoni and Socolow, 2013, Wiltshire and Davies-Barnard, 2015); the C uptake

simulated by the LUMs is only achieved in one out of 16 combinations of mitigation LUC scenarios and DGVMs. The main reasons for the typically lower C uptake in the DGVMs as initially implemented in the LUMs are slower soil C accumulation (or even losses) following afforestation, different assumptions on potential vegetation C stocks, lower growth rates of forests, and lower bioenergy yields. Clearly the per-area C uptake (and thus the land demand) in land-based mitigation scenarios depends on assumptions made about vegetation and soil processes in the IAMs/LUMs. An improved implementation of land-based CDR options in both kinds of models, LUMs and DGVMs, as well as a deeper interaction between both is necessary to draw more robust conclusions about the potential contribution of land management to climate stabilization. While the LUMs should emphasize the large uncertainty in assumed yields from bioenergy plantations, the DGVMs need to improve the parameterizations of managed herbaceous vegetation, particularly bioenergy crops (and also woody bioenergy), as well as regrowth of managed forests for afforestation. Field observations should focus on studying bioenergy crop productivity under commercial production conditions. Additionally, the LUMs and some DGVMs need to reconsider their assumptions about soil C sequestration rates following afforestation. More detailed information about grazing intensities on grasslands, and a clear differentiation between natural grasslands and intensively managed pastures in observational studies might also help to reduce the uncertainty in soil C changes following LUC (Navarrete *et al.*, 2016).

In this study we only address the uncertainty in land-based mitigation arising from potential C uptake for a prescribed available area. However, the establishment of negative emissions from land management could also be hindered by unacceptable social or ecological side-effects (Kartha and Dooley, 2016, Krause *et al.*, 2017, Smith *et al.*, 2016a), biophysical and biogeochemical climate impacts beyond C (Boysen *et al.*, 2017a, Krause *et al.*, 2017, Smith

et al., 2016a), irreversible effects of overshooting CO_2 concentrations (Kartha and Dooley, 2016, Tokarska and Zickfeld, 2015), or simply because CCS turns out to be technologically infeasible at commercial scale. There is also strong evidence that the timescales for shifts in farming systems to be realized may be of the order of several decades, substantially delaying the onset of negative emissions from BECCS (Alexander *et al.*, 2013; Brown et al., submitted). Combining these unknowns and caveats with the large uncertainty in uptake potential identified in this study suggests that relying on negative emissions to mitigate climate change is a very high-risk strategy.

Acknowledgements

This work was funded by the Helmholtz Association through the International Research Group CLUCIE and by the European Commission's Seventh Framework Programme, under grant agreement number 603542 (LUC4C). Andreas Krause, Anita D. Bayer, and Almut Arneth also acknowledge support by the European Commission's Seventh Framework Programme, under grant agreement number 308393 (OPERAs). This work was supported, in part, by the German Federal Ministry of Education and Research (BMBF), through the Helmholtz Association and its research program ATMO. It also represents paper number 22 of the Birmingham Institute of Forest Research.

Conflict of Interest

The authors declare no conflict of interest.

References

Alexander P, Moran D, Rounsevell MDA, Smith P (2013) Modelling the perennial energy crop market: the role of spatial diffusion. *Journal of the Royal Society Interface,* **10**, doi:10.1098/Rsif.2013.0656.

Alexandratos N, Bruinsma J (2012) World agriculture towards 2030/2050: the 2012 revision. Rome, FAO.

Anav A, Friedlingstein P, Kidston M *et al.* (2013) Evaluating the Land and Ocean Components of the Global Carbon Cycle in the CMIP5 Earth System Models. *Journal of Climate,* **26**, 6801-6843, doi:10.1175/Jcli-D-12-00417.1.

Anderson-Teixeira KJ, Wang MMH, Mcgarvey JC, Lebauer DS (2016) Carbon dynamics of mature and regrowth tropical forests derived from a pantropical database (TropForC-db). *Global Change Biology,* **22**, 1690-1709, doi:10.1111/gcb.13226.

Anderson K, Peters G (2016) The trouble with negative emissions. *Science,* **354**, 182-183, doi:10.1126/science.aah4567.

Arneth A, Sitch S, Pongratz J *et al.* (2017) Historical carbon dioxide emissions caused by land-use changes are possibly larger than assumed. *Nature Geoscience,* **10**, 79-84, doi:10.1038/NGEO2882.

Asner GP, Powell GVN, Mascaro J *et al.* (2010) High-resolution forest carbon stocks and emissions in the Amazon. *Proceedings of the National Academy of Sciences of the United States of America,* **107**, 16738-16742, doi:10.1073/pnas.1004875107.

Bayer AD, Lindeskog M, Pugh TaM, Anthoni PM, Fuchs R, Arneth A (2017) Uncertainties in the land-use flux resulting from land-use change reconstructions and gross land transitions. *Earth System Dynamics,* **8**, 91-111, doi:10.5194/esd-8-91-2017.

Best MJ, Pryor M, Clark DB *et al.* (2011) The Joint UK Land Environment Simulator (JULES), model description - Part 1: Energy and water fluxes. *Geoscientific Model Development,* **4**, 677-699, doi:10.5194/gmd-4-677-2011.

Bondeau A, Smith PC, Zaehle S *et al.* (2007) Modelling the role of agriculture for the 20th century global terrestrial carbon balance. *Global Change Biology,* **13**, 679-706, doi:10.1111/j.1365-2486.2006.01305.x.

Boysen LR, Lucht W, Gerten D (2017a) Trade-offs for food production, nature conservation and climate limit the terrestrial carbon dioxide removal potential. *Global Change Biology*, doi:10.1111/gcb.13745.

Boysen LR, Lucht W, Gerten D, Heck V, Lenton TM, Schellnhuber HJ (2017b) The limits to global-warming mitigation by terrestrial carbon removal. *Earths Future,* **5**, 463-474, doi:10.1002/2016EF000469.

Cairns MA, Brown S, Helmer EH, Baumgardner GA (1997) Root biomass allocation in the world's upland forests. *Oecologia,* **111**, 1-11, doi:10.1007/s004420050201.

Ciais P, Wattenbach M, Vuichard N *et al.* (2010) The European carbon balance. Part 2: croplands. *Global Change Biology,* **16**, 1409-1428, doi:10.1111/j.1365-2486.2009.02055.x.

Clark DB, Mercado LM, Sitch S *et al.* (2011) The Joint UK Land Environment Simulator (JULES), model description - Part 2: Carbon fluxes and vegetation dynamics. *Geoscientific Model Development,* **4**, 701-722, doi:10.5194/gmd-4-701-2011.

Cleveland CC, Taylor P, Chadwick KD *et al.* (2015) A comparison of plot-based satellite and Earth system model estimates of tropical forest net primary production. *Global Biogeochemical Cycles,* **29**, 626-644, doi:10.1002/2014GB005022.

Creutzig F (2016) Economic and ecological views on climate change mitigation with bioenergy and negative emissions. *Global Change Biology Bioenergy,* **8**, 4-10, doi:10.1111/gcbb.12235.

Defries R (2002) Past and future sensitivity of primary production to human modification of the landscape. *Geophysical Research Letters,* **29**, doi:10.1029/2001gl013620.

Deng L, Zhu G, Tang Z, Shangguan Z (2016) Global patterns of the effects of land-use changes on soil carbon stocks. *Global Ecology and Conservation,* **5**, 127-138, doi:10.1016/j.gecco.2015.12.004.

Doelman JC, Stehfest E, Tabeau A *et al.* (2018) Exploring SSP land-use dynamics using the IMAGE model: Regional and gridded scenarios of land-use change and land-based climate change mitigation. *Global Environmental Change,* **48**, 119-135, doi:10.1016/j.gloenvcha.2017.11.014.

Don A, Schumacher J, Freibauer A (2011) Impact of tropical land-use change on soil organic carbon stocks - a meta-analysis. *Global Change Biology,* **17**, 1658-1670, doi:10.1111/j.1365-2486.2010.02336.x.

Fargione J, Hill J, Tilman D, Polasky S, Hawthorne P (2008) Land clearing and the biofuel carbon debt. *Science,* **319**, 1235-1238, doi:10.1126/science.1152747.

Fuss S, Canadell JG, Peters GP *et al.* (2014) COMMENTARY: Betting on negative emissions. *Nature Climate Change,* **4**, 850-853, doi:10.1038/nclimate2392.

Gasser T, Guivarch C, Tachiiri K, Jones CD, Ciais P (2015) Negative emissions physically needed to keep global warming below 2 degrees C. *Nature Communications,* **6**, doi:10.1038/Ncomms8958.

Guo LB, Gifford RM (2002) Soil carbon stocks and land use change: a meta analysis. *Global Change Biology,* **8**, 345-360, doi:10.1046/j.1354-1013.2002.00486.x.

Heck V, Gerten D, Lucht W, Boysen LR (2016) Is extensive terrestrial carbon dioxide removal a 'green' form of geoengineering? A global modelling study. *Global and Planetary Change,* **137**, 123-130, doi:10.1016/j.gloplacha.2015.12.008.

Hempel S, Frieler K, Warszawski L, Schewe J, Piontek F (2013) A trend-preserving bias correction - the ISI-MIP approach. *Earth System Dynamics,* **4**, 219-236, doi:10.5194/esd-4-219-2013.

Houghton RA, Nassikas AA (2017) Negative emissions from stopping deforestation and forest degradation, globally. *Global Change Biology*, 1-10, doi:10.1111/gcb.13876.

Humpenöder F, Popp A, Dietrich JP *et al.* (2014) Investigating afforestation and bioenergy CCS as climate change mitigation strategies. *Environmental Research Letters,* **9**, doi:10.1088/1748-9326/9/6/064029.

Johnson MO, Galbraith D, Gloor M *et al.* (2016) Variation in stem mortality rates determines patterns of above-ground biomass in Amazonian forests: implications for dynamic global vegetation models. *Global Change Biology,* **22**, 3996-4013, doi:10.1111/gcb.13315.

Kartha S, Dooley K (2016) The risks of relying on tomorrow's 'negative emissions' to guide today's mitigation action. Stockholm Environment Institute.

Klein D, Luderer G, Kriegler E *et al.* (2014) The value of bioenergy in low stabilization scenarios: an assessment using REMIND-MAgPIE. *Climatic Change,* **123**, 705-718, doi:10.1007/s10584-013-0940-z.

Klein Goldewijk K, Beusen A, Van Drecht G, De Vos M (2011) The HYDE 3.1 spatially explicit database of human-induced global land-use change over the past 12,000 years. *Global Ecology and Biogeography,* **20**, 73-86, doi:10.1111/j.1466-8238.2010.00587.x.

Krause A, Pugh TaM, Bayer AD *et al.* (2017) Global consequences of afforestation and bioenergy cultivation on ecosystem service indicators. *Biogeosciences,* **14**, 4829–4850, doi:10.5194/bg-14-4829-2017.

Krause A, Pugh TaM, Bayer AD, Lindeskog M, Arneth A (2016) Impacts of land-use history on the recovery of ecosystems after agricultural abandonment. *Earth System Dynamics,* **7**, 745-766, doi:10.5194/esd-7-745-2016.

Krinner G, Viovy N, De Noblet-Ducoudre N *et al.* (2005) A dynamic global vegetation model for studies of the coupled atmosphere-biosphere system. *Global Biogeochemical Cycles,* **19**, doi:10.1029/2003gb002199.

Laganiere J, Angers DA, Pare D (2010) Carbon accumulation in agricultural soils after afforestation: a meta-analysis. *Global Change Biology,* **16**, 439-453, doi:10.1111/j.1365-2486.2009.01930.x.

Le Quere C, Andrew RM, Canadell JG *et al.* (2016) Global Carbon Budget 2016. *Earth System Science Data,* **8**, 605-649, doi:10.5194/essd-8-605-2016.

Lenton TM (2010) The potential for land-based biological CO2 removal to lower future atmospheric CO2 concentration. *Carbon Management,* **1**, 145-160, doi:10.4155/Cmt.10.12.

Lenton TM, Vaughan NE (2009) The radiative forcing potential of different climate geoengineering options. *Atmospheric Chemistry and Physics,* **9**, 5539-5561, doi:10.5194/acp-9-5539-2009.

Lotze-Campen H, Muller C, Bondeau A, Rost S, Popp A, Lucht W (2008) Global food demand, productivity growth, and the scarcity of land and water resources: a spatially explicit mathematical programming approach. *Agricultural Economics,* **39**, 325-338, doi:10.1111/j.1574-0862.2008.00336.x.

Luyssaert S, Ciais P, Piao SL *et al.* (2010) The European carbon balance. Part 3: forests. *Global Change Biology,* **16**, 1429-1450, doi:10.1111/j.1365-2486.2009.02056.x.

Martin PA, Newton AC, Bullock JM (2013) Carbon pools recover more quickly than plant biodiversity in tropical secondary forests. *Proceedings of the Royal Society B-Biological Sciences,* **280**, doi:10.1098/Rspb.2013.2236.

Mcsherry ME, Ritchie ME (2013) Effects of grazing on grassland soil carbon: a global review. *Global Change Biology,* **19**, 1347-1357, doi:10.1111/gcb.12144.

Meinshausen M, Smith SJ, Calvin K *et al.* (2011) The RCP greenhouse gas concentrations and their extensions from 1765 to 2300. *Climatic Change,* **109**, 213-241, doi:10.1007/s10584-011-0156-z.

Monfreda C, Ramankutty N, Foley JA (2008) Farming the planet: 2. Geographic distribution of crop areas, yields, physiological types, and net primary production in the year 2000. *Global Biogeochemical Cycles,* **22**, doi:10.1029/2007gb002947.

Navarrete D, Sitch S, Aragao LEOC, Pedroni L (2016) Conversion from forests to pastures in the Colombian Amazon leads to contrasting soil carbon dynamics depending on land management practices. *Global Change Biology,* **22**, 3503-3517, doi:10.1111/gcb.13266.

Olin S, Lindeskog M, Pugh TaM *et al.* (2015) Soil carbon management in large-scale Earth system modelling: implications for crop yields and nitrogen leaching. *Earth System Dynamics,* **6**, 745-768, doi:10.5194/esd-6-745-2015.

Paul KI, Polglase PJ, Nyakuengama JG, Khanna PK (2002) Change in soil carbon following afforestation. *Forest Ecology and Management,* **168**, 241-257, doi:10.1016/S0378-1127(01)00740-X.

Poeplau C, Don A, Vesterdal L, Leifeld J, Van Wesemael B, Schumacher J, Gensior A (2011) Temporal dynamics of soil organic carbon after land-use change in the temperate zone - carbon response functions as a model approach. *Global Change Biology,* **17**, 2415-2427, doi:10.1111/j.1365-2486.2011.02408.x.

Poorter L, Ongers FB, Aide TM *et al.* (2016) Biomass resilience of Neotropical secondary forests. *Nature,* **530**, 211-214, doi:10.1038/nature16512.

Popp A, Calvin K, Fujimori S *et al.* (2017) Land-use futures in the shared socio-economic pathways. *Global Environmental Change-Human and Policy Dimensions,* **42**, 331-345, doi:10.1016/j.gloenvcha.2016.10.002.

Popp A, Humpenoder F, Weindl I *et al.* (2014a) Land-use protection for climate change mitigation. *Nature Climate Change,* **4**, 1095-1098, doi:10.1038/Nclimate2444.

Popp A, Rose SK, Calvin K *et al.* (2014b) Land-use transition for bioenergy and climate stabilization: model comparison of drivers, impacts and interactions with other land use based mitigation options. *Climatic Change,* **123**, 495-509, doi:10.1007/s10584-013-0926-x.

Powers JS, Corre MD, Twine TE, Veldkamp E (2011) Geographic bias of field observations of soil carbon stocks with tropical land-use changes precludes spatial extrapolation. *Proceedings of*

the National Academy of Sciences of the United States of America, **108**, 6318-6322, doi:10.1073/pnas.1016774108.

Pugh TaM, Arneth A, Olin S *et al.* (2015) Simulated carbon emissions from land use change are substantially enhanced by accounting for agricultural management. *Environmental Research Letters,* **10**, doi:10.1088/1748-9326/10/12/124008.

Riahi K, Van Vuuren DP, Kriegler E *et al.* (2017) The Shared Socioeconomic Pathways and their energy, land use, and greenhouse gas emissions implications: An overview. *Global Environmental Change-Human and Policy Dimensions,* **42**, 153-168, doi:10.1016/j.gloenvcha.2016.05.009.

Rogelj J, Luderer G, Pietzcker RC, Kriegler E, Schaeffer M, Krey V, Riahi K (2015) Energy system transformations for limiting end-of-century warming to below 1.5 degrees C. *Nature Climate Change,* **5**, 519–527, doi:10.1038/nclimate2572.

Sanderman J, Hengl T, Fiske GJ (2017) Soil carbon debt of 12,000 years of human land use. *Proceedings of the National Academy of Sciences of the United States of America,* **114**, 9575-9580, doi:10.1073/pnas.1706103114.

Sanderson BM, O'neill BC, Tebaldi C (2016) What would it take to achieve the Paris temperature targets? *Geophysical Research Letters,* **43**, 7133-7142, doi:10.1002/2016GL069563.

Scharlemann JPW, Tanner EVJ, Hiederer R, Kapos V (2014) Global soil carbon: understanding and managing the largest terrestrial carbon pool. *Carbon Management,* **5**, 81-91, doi:10.4155/Cmt.13.77.

Searle SY, Malins CJ (2014) Will energy crop yields meet expectations? *Biomass & Bioenergy,* **65**, 3-12, doi:10.1016/j.biombioe.2014.01.001.

Silver WL, Ostertag R, Lugo AE (2000) The potential for carbon sequestration through reforestation of abandoned tropical agricultural and pasture lands. *Restoration Ecology,* **8**, 394-407, doi:10.1046/j.1526-100x.2000.80054.x.

Sitch S, Smith B, Prentice IC *et al.* (2003) Evaluation of ecosystem dynamics, plant geography and terrestrial carbon cycling in the LPJ dynamic global vegetation model. *Global Change Biology,* **9**, 161-185, doi:10.1046/j.1365-2486.2003.00569.x.

Smith B, Warlind D, Arneth A, Hickler T, Leadley P, Siltberg J, Zaehle S (2014) Implications of incorporating N cycling and N limitations on primary production in an individual-based dynamic vegetation model. *Biogeosciences,* **11**, 2027-2054, doi:10.5194/bg-11-2027-2014.

Smith P, Davis SJ, Creutzig F *et al.* (2016a) Biophysical and economic limits to negative CO2 emissions. *Nature Climate Change,* **6**, 42-50, doi:10.1038/Nclimate2870.

Smith P, House JI, Bustamante M *et al.* (2016b) Global change pressures on soils from land use and management. *Global Change Biology,* **22**, 1008-1028, doi:10.1111/gcb.13068.

Sonntag S, Pongratz J, Reick CH, Schmidt H (2016) Reforestation in a high-CO2 world-Higher mitigation potential than expected, lower adaptation potential than hoped for. *Geophysical Research Letters,* **43**, 6546-6553, doi:10.1002/2016GL068824.

Stehfest E, Van Vuuren D, Kram T *et al.* (2014) Integrated Assessment of Global Environmental Change with IMAGE 3.0 : Model description and policy applications. The Hague: PBL Netherlands Environmental Assessment Agency.

Tavoni M, Socolow R (2013) Modeling meets science and technology: an introduction to a special issue on negative emissions. *Climatic Change,* **118**, 1-14, doi:10.1007/s10584-013-0757-9.

Tian HQ, Lu CQ, Yang J *et al.* (2015) Global patterns and controls of soil organic carbon dynamics as simulated by multiple terrestrial biosphere models: Current status and future directions. *Global Biogeochemical Cycles,* **29**, 775-792, doi:10.1002/2014GB005021.

Todd-Brown KEO, Randerson JT, Post WM, Hoffman FM, Tarnocai C, Schuur EaG, Allison SD (2013) Causes of variation in soil carbon simulations from CMIP5 Earth system models and comparison with observations. *Biogeosciences,* **10**, 1717-1736, doi:10.5194/bg-10-1717-2013.

Tokarska KB, Zickfeld K (2015) The effectiveness of net negative carbon dioxide emissions in reversing anthropogenic climate change. *Environmental Research Letters,* **10**, doi:10.1088/1748-9326/10/9/094013.

Williamson P (2016) Scrutinize CO2 removal methods. *Nature,* **530**, 153-155, doi:10.1038/530153a.

Wiltshire A, Davies-Barnard T (2015) Planetary limits to BECCS negative emissions. In: *AVOID 2 WPD.2a Report 1.*

Tables

Table 1: Overview of major DGVM differences relevant to this study. A more detailed version of the table can be found in the supplement (Table S1).

Variable or process	DGVM			
	LPJ-GUESS	ORCHIDEE	JULES	LPJmL
Spatial resolution	0.5° x 0.5°	2° x 2°	0.5° x 0.5°	
Nitrogen cycle	yes	no		
Implementation of LU patterns from the LUMs into the DGVM	absolute cropland, pasture, and natural area prescribed by LUMs, PFT distribution on natural land is simulated dynamically	changes in cropland, pasture, and forest vs. other natural area prescribed by LUMs, forest area and PFT distribution (static on natural land) in year 2005 according to internal map (from European Space Agency)	absolute cropland, pasture, and natural area prescribed by LUMs, PFT distribution on natural land is simulated dynamically	
Implementation of agricultural expansion	all natural PFTs are reduced proportionally		grasslands are reduced first, then shrubs, then forests	all natural PFTs are reduced proportionally
Representation of degraded forests (for IMAGE-LU patterns only)	as pasture	as natural grassland	as natural vegetation (forests or natural grassland)	as pasture
Forest (re)growth dynamics	cohort approach (competition between different age classes), natural regrowth	dilution approach (one average individual per PFT), natural regrowth		
Pasture management	harvest, woody vegetation is prevented from growing	no harvest, woody vegetation is prevented from growing	harvest*, woody vegetation is prevented from growing	harvest with variable intensity, woody vegetation is

				prevented from growing
Cropland management	four crop PFTs (temperate wheat, maize, rice, temperate other), variable sowing and harvest date, tillage, irrigation, fertilization, dynamic potential heat unit calculation, woody vegetation is prevented from growing	C3 + C4 crop grass (similar phenology as natural grass but adapted maximum LAI and slightly modified critical temperature and humidity parameters), harvest, woody vegetation is prevented from growing	C3 + C4 grass, harvest, woody vegetation is prevented from growing	12 crop PFTs, variable sowing and harvest date, irrigation, woody vegetation is prevented from growing
Dedicated bioenergy crop PFTs	no (grown as maize)	no (grown as C3 or C4 crop grass)	no (grown as C3 or C4 grass)	yes (fast-growing C4 grass, temperate and tropical short rotation coppices)

*Pastures were treated as cropland in these JULES simulations. Normally pastures are not harvested in JULES.

Figure captions

Figure 1: Time-series (2010-2099) of simulated C uptake (total of all grid-cells) in the LUMs and DGVMs for the mitigation simulations (compared to the respective BASE simulation), for IMAGE-LU patterns (left, 5-year running means) and MAgPIE-LU patterns (right). a+b) total C (including cumulative CCS), c+d) vegetation C, e+f) litter and soil C, g+h) cumulative CCS.

Figure 2: Simulated change in total C (a), vegetation C (b), litter and soil C (c), cumulative CCS (d), cumulative instant (oxidized in the same year) deforestation/degradation emissions (e), and cumulative NPP (f) between year 2005 and 2099 for the mitigation simulations (compared to the respective BASE simulation) in IMAGE/MAgPIE (as simulated by the LUMs in the LUC scenarios), LPJ-GUESS, ORCHIDEE, JULES and LPJmL.

Figure 3: Spatial distribution of total C uptake in the LUMs (a-d) and DGVMs (e-t) for the mitigation scenarios (compared to BASE) between year 2005 and 2099 for IMAGE ADAFF (1^{st} column), MAgPIE ADAFF (2^{nd} column), IMAGE BECCS (3^{rd} column) and MAgPIE BECCS (4^{th} column). Numbers are global totals.

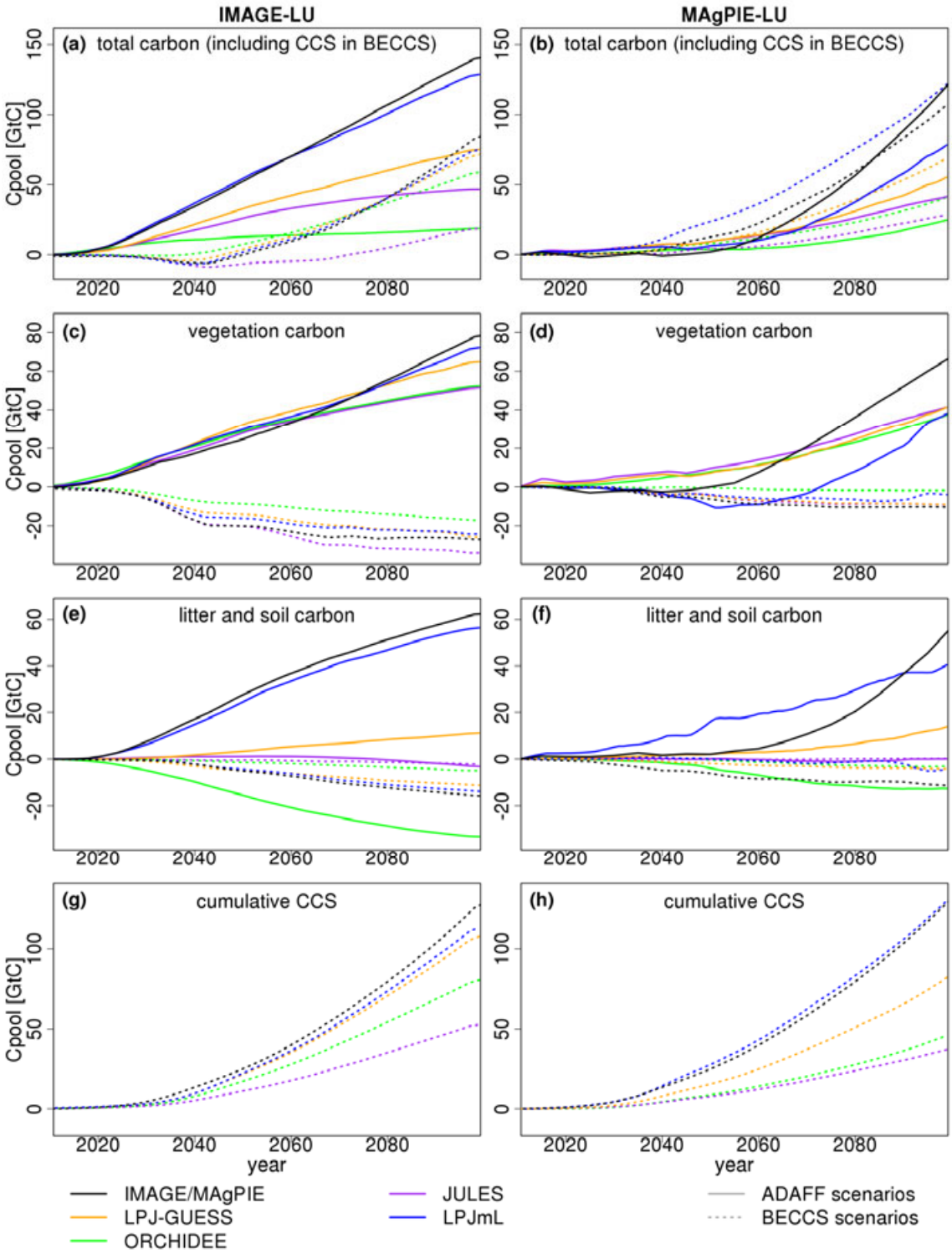
IMAGE-LU
MAgPIE-LU
(a) total carbon (including CCS in BECCS)
(b) total carbon (including CCS in BECCS)
(c) vegetation carbon
(d) vegetation carbon
(e) litter and soil carbon
(f) litter and soil carbon
(g) cumulative CCS
(h) cumulative CCS
Cpool [GtC]
year
IMAGE/MAgPIE
LPJ-GUESS
ORCHIDEE
JULES
LPJmL
ADAFF scenarios
BECCS scenarios

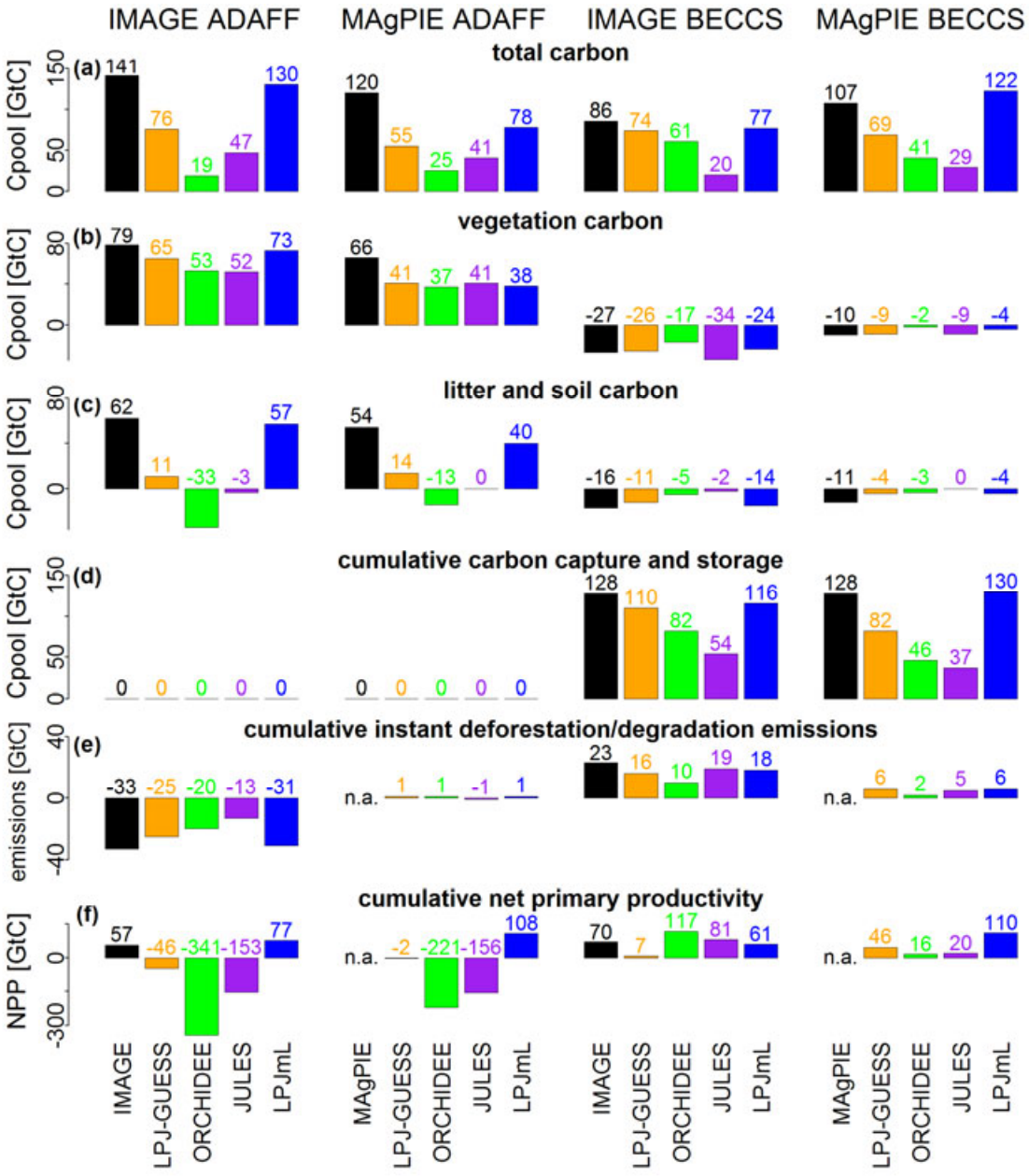
IMAGE ADAFF
MAgPIE ADAFF
IMAGE BECCS
MAgPIE BECCS
total carbon
(a)
Cpool [GtC]
141 76 19 47 130
120 55 25 41 78
86 74 61 20 77
107 69 41 29 122
vegetation carbon
(b)
79 65 53 52 73
66 41 37 41 38
-27 -26 -17 -34 -24
-10 -9 -2 -9 -4
litter and soil carbon
(c)
62 11 -33 -3 57
54 14 -13 0 40
-16 -11 -5 -2 -14
-11 -4 -3 0 -4
cumulative carbon capture and storage
(d)
0 0 0 0 0
0 0 0 0 0
128 110 82 54 116
128 82 46 37 130
cumulative instant deforestation/degradation emissions
(e)
emissions [GtC]
-33 -25 -20 -13 -31
n.a. 1 1 -1 1
23 16 10 19 18
n.a. 6 2 5 6
cumulative net primary productivity
(f)
NPP [GtC]
57 -46 -341 -153 77
n.a. -2 -221 -156 108
70 7 117 81 61
n.a. 46 16 20 110
IMAGE
LPJ-GUESS
ORCHIDEE
JULES
LPJmL
MAgPIE
LPJ-GUESS
ORCHIDEE
JULES
LPJmL
IMAGE
LPJ-GUESS
ORCHIDEE
JULES
LPJmL
MAgPIE
LPJ-GUESS
ORCHIDEE
JULES
LPJmL

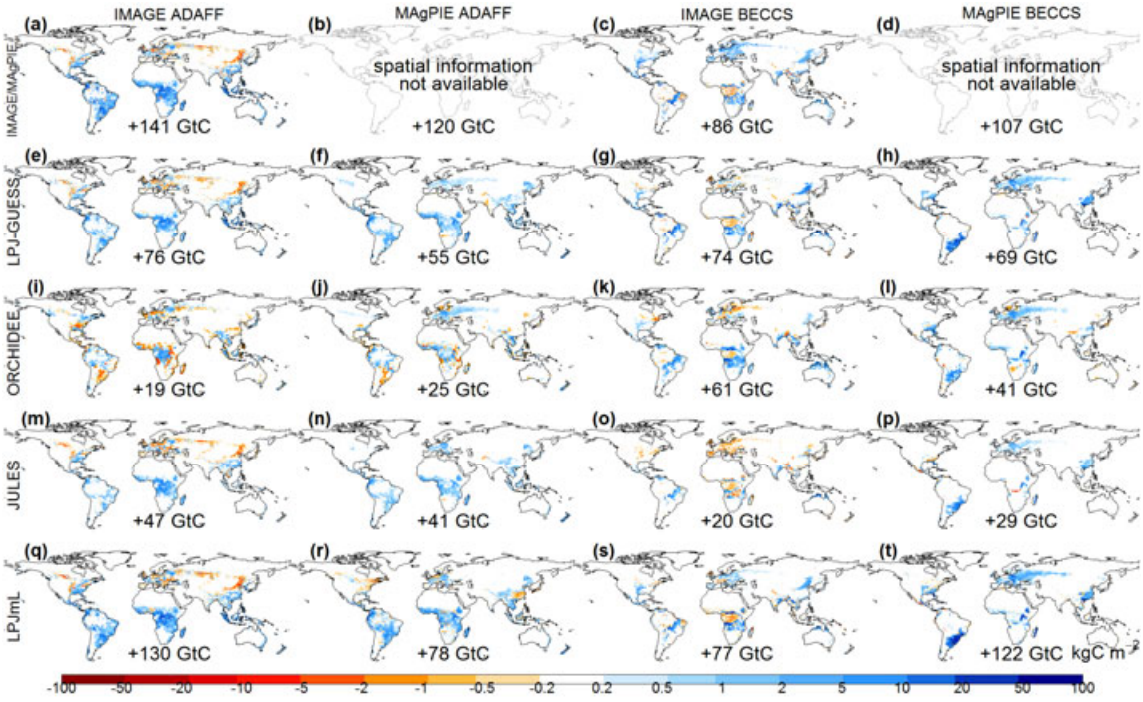
IMAGE ADAFF
MAgPIE ADAFF
IMAGE BECCS
MAgPIE BECCS
IMAGE/MAgPIE
LPJ-GUESS
ORCHIDEE
JULES
LPJmL
(a)
(b)
(c)
(d)
(e)
(f)
(g)
(h)
(i)
(j)
(k)
(l)
(m)
(n)
(o)
(p)
(q)
(r)
(s)
(t)
spatial information not available
spatial information not available
+141 GtC
+120 GtC
+86 GtC
+107 GtC
+76 GtC
+55 GtC
+74 GtC
+69 GtC
+19 GtC
+25 GtC
+61 GtC
+41 GtC
+47 GtC
+41 GtC
+20 GtC
+29 GtC
+130 GtC
+78 GtC
+77 GtC
+122 GtC
kgC m-2
-100
-50
-20
-10
-5
-2
-1
-0.5
-0.2
0.2
0.5
1
2
5
10
20
50
100